



OPEN Improved biosynthesis and characteristics of silver nanoparticles using marine endophytic fungi exposed to hypo-osmotic stress

Miguel A. M. Oliveira¹, Maria L. Calado¹, Sara F. C. Guerreiro^{2,3,4,5}, Juliana R. Dias², Maria J. Campos¹, Patrick G. Murray⁶ & Sara C. Novais¹✉

Silver nanoparticles (AgNPs) are valued for their unique properties and can be synthesized biologically, offering a greener alternative to traditional methods. This study assessed the potential of cell-free filtrates (CFFs) of seaweed-associated marine fungi to produce AgNPs. More specifically, *Talaromyces pinophilus*, *Aspergillus fructus*, *Stemphylium gracilariae*, *Purpureocillium lilacinum*, *Microascus croci*, *Penicillium toxicarium*, *Exophiala mesophila*, and *Emericellopsis maritima*, when cultured in media prepared with artificial seawater or distilled water (hypo-osmotic conditions) as a possible stress inducer. Optimization of the reaction conditions including changes in pH, temperature, reaction time, and the concentration of AgNO₃ and CFF were evaluated for obtaining high relative concentrations and theoretically small sized AgNPs. High pH (10), elevated temperature (100 °C), and the highest AgNO₃ concentration tested (1.5 mM) were found to be key. Moreover, CFFs from marine endophytic fungi grown under hypo-osmotic conditions, in particular *T. pinophilus*, *A. fructus*, *P. lilacinum*, *P. toxicarium*, and *E. maritima*, biosynthesized higher relative concentrations of generally monodispersed AgNPs with moderate stability (zeta-potential between – 20 and – 30 mV) and varying nanoparticle average sizes (between 40.64 and 191.60 nm) with high percentages of very small particles (below 50 nm). This study demonstrates the potential of marine endophytic fungi for AgNPs biosynthesis, showing that modifying fungal growth conditions enhances green AgNPs production. Future research on diverse stress conditions may further optimize this eco-friendly approach.

Keywords Cell-free filtrate, Fungal mediated synthesis, Green synthesis, Nanotechnology, Response surface methodology

Silver nanoparticles (AgNPs) are a sought-after nanomaterial due to their numerous application possibilities. AgNPs, in the 1–100 nm size range, are very prominent in the nanotech industry due to their unique physicochemical characteristics (e.g., size, shape, morphology) that confer them specific biological properties (e.g., antimicrobial, anticancer, anti-inflammatory)^{1,2}.

AgNPs can be synthesized by traditional physicochemical methods or through biological processes, which can be generally classified into top-down (bulk materials are broken down) and bottom-up (atoms and molecules are combined) approaches³. Traditional production of AgNPs (e.g., laser ablation, chemical reduction) can

¹MARE - Marine and Environmental Sciences Centre & ARNET - Aquatic Research Network, ESTM, Polytechnic University of Leiria, Edifício CETEMARES, Avenida do Porto de Pesca, 2520-630 Peniche, Portugal. ²Centre for Rapid and Sustainable Product Development, Polytechnic University of Leiria, 2430-028 Marinha Grande, Portugal. ³Medical Physics, Radiobiology and Radiation Protection Group, IPO Porto Research Center (CI-IPO), Portuguese Oncology Institute of Porto (IPO/Porto)/Porto Comprehensive Cancer Centre (Porto.CCC) & RISE@CI-IPO (Health Research Network), R. Dr. António Bernardino de Almeida, 4200-072 Porto, Portugal. ⁴i3S - Instituto de Investigação e Inovação em Saúde, Universidade do Porto, R. Alfredo Allen 208, 4200-135 Porto, Portugal. ⁵FEUP - Faculdade de Engenharia da Universidade do Porto, R. Dr. Roberto Frias, s/n, 4200-135 Porto, Portugal. ⁶LIFE - Health and Biosciences Research Institute, Technological University of the Shannon, Limerick V94EC5T, Ireland. ✉email: sara.novais@ipleiria.pt

often be expensive and can release harmful chemicals into the environment particularly in the stabilization steps¹. Therefore, alternative methods are being explored to reduce these negative impacts. The biosynthesis of nanoparticles has attracted growing interest as a more environmentally friendly alternative aligned with the principles of green chemistry². This innovative approach is simpler, reliable, cost-effective, environmentally beneficial and allows the production of a high yield of colloidal AgNPs with defined size and morphology and reasonable stability and longevity in mild reaction conditions^{1,2,4}. AgNPs biosynthesis can be facilitated by both multicellular and unicellular organisms from terrestrial and marine environments. Biological extracts from these organisms can act as efficient capping and reducing agents³. Biosynthesized AgNPs have been shown to exhibit significant bioactive properties, including antimicrobial, antioxidant, antibiofilm, and anticancer activities⁵.

The use of fungal biomass or their cell-free filtrates (CFFs), is an efficient and cost-effective approach that enables large-scale production due to fast mycelial growth, low subproducts toxicity and high production of unique metabolites that can enhance AgNPs stability, biological activity, and production yield^{3,6,7}. The fungal system can be used for intracellular (incorporation of the metal precursor into the mycelium) or extracellular (addition of the metal precursor to the CFF) biosynthesis, being the later the most used^{3,6}. The biosynthesis reaction varies greatly with the fungal species used, as different species produce distinct metabolites, but also with culturing and synthesis conditions, such as temperature, pH, and metal salt precursor concentrations, resulting in AgNPs with different characteristics^{6,7}.

Fungi that occur in marine environments, associated with various marine hosts or substrates, have recently become the focus of bioprospecting studies⁸. Marine endophytic fungi, and particularly those colonizing the internal tissues of seaweed in an apparent beneficial relationship, have been shown to be capable of producing chemically new and structurally unique compounds with several biotechnological applications^{9,10}. There are relatively few studies showing the ability of marine fungi CFFs to produce AgNPs, with the first one being published in 2009, and even less with marine fungi associated with seaweed^{11–14}. Moreover, there is limited information on optimal conditions for AgNPs with ideal yield, size, and stability, as fungal species, culturing and reaction conditions affect metabolite production, influencing these characteristics.

Thus, the main objective of this work was to assess the capacity of different marine fungal species' cell-free filtrates to synthesize colloidal AgNPs with optimal size, yield, dispersity, and stability. To achieve this goal the following specific objectives were pursued: (1) to isolate marine endophytic fungi associated with seaweeds and evaluate their growth rates under different culture conditions (presence and absence of salt in the culture medium as potential hypo-osmotic stress induction); (2) to access the capacity of the cell-free filtrates to synthesize silver nanoparticles, optimizing synthesis conditions.

Methods

Isolation of marine endophytic fungi from different seaweed hosts

Attached and healthy thalli of five species of seaweed—*Corallina elongata* J.Ellis & Solander, 1786, *Cystoseira tamariscifolia* (Hudson) Papenfuss, 1950, *Fucus guiryi* Zardi, Nicastro, E.S.Serrão & G.A.Pearson, 2011, *Sargassum cf. muticum* (Yendo) Fensholt, 1955, and *Stypocaulon scoparium* (Linnaeus) Kützting, 1843—were collected from a sandy beach in Leça da Palmeira (41.1883°N, 8.7070°W) and two sandy beaches in the Peniche peninsula (Gambôa: 39.3651°N, 9.3728°W; Portinho da Areia Norte: 39.3691°N, 9.3779°W) from May to October 2018. In the laboratory, the algal samples were carefully rinsed with sterile seawater and their surfaces were sterilized to ensure the exclusive isolation of endophytes. Each sample was aseptically cut into small segments and inoculated onto two culture media, malt extract agar [malt extract (30 g/L; VWR Chemicals, Radnor, Pennsylvania, USA), peptone (5 g/L; VWR Chemicals) and agar (15 g/L; Liofilchem, Italy)] and corn meal agar [corn meal (50 g/L; Sigma-Aldrich, St. Louis, Missouri, USA) and agar (15 g/L; Liofilchem)] prepared with sterile seawater, supplemented with chloramphenicol (Sigma-Aldrich) at a concentration of 200 mg/L. The plates were incubated at 28 °C, in the dark, and monitored daily for the emergence of new hyphae from the inner algal tissue. Each fungal strain was then transferred to a new plate with potato dextrose agar medium [potato dextrose (24 g/L; VWR Chemicals) and agar (15 g/L; Liofilchem)] and followed sequential inoculations to obtain a pure culture. Once a pure culture was established for every isolate, the biological material proceeded to molecular identification.

Molecular identification of marine fungal isolates

Based on preliminary assays on the potential of the isolated fungal strains for AgNPs biosynthesis (data not shown), and with the aim of including at least one species from each seaweed source, eight out of the eighteen strains isolated were molecularly identified and further tested. The identification method involved extracting genomic DNA using an optimized phenol–chloroform protocol¹⁵, followed by amplification and sequencing of internal transcribed spacers (ITS) 1 and 2, along with the intervening 5.8S region of nuclear ribosomal DNA, using the primer pair ITS5 and ITS4¹⁶. Additional genes were also amplified and sequenced for the identifications of specific fungal groups, to enable the identification to the species level. The following primers pairs were used in this study: T1/Bt2b and Bt2a/Bt2b for partial β -tubulin gene of *Emericellopsis*, and *Microascus*, *Penicillium*, and *Talaromyces* genera, respectively^{17–20}; RPB2-5F/RPB2-7CR for RNA polymerase II (RPB2) gene of *Emericellopsis* and *Penicillium* genera^{17,21}; CALDF1/CALDR and CMD5/CMD6 for partial calmodulin (cal) gene of *Stemphylium*, and *Aspergillus* and *Penicillium*, respectively^{17,22,23}; and EF1-983/EF1-2218r for partial translation elongation factor 1-alpha (tef1- α) gene of *Emericellopsis* and *Microascus* genera^{20,21}. The conditions of polymerase chain reactions (PCR) and purification of PCR products are described in¹⁰. The DNA sequences of the isolates were compared with those published in the National Center for Biotechnology Information (NCBI) database and identified to the lowest taxonomic level possible. The identification of one of the fungal isolates required a multilocus phylogenetic analysis, using the genes that presented higher phylogenetic signal. This analysis was performed with the aligned sequences of different genes/regions from the isolate and closely related

species, involving the construction of a phylogenetic tree based on maximum Likelihood (ML) criteria. ML analysis was based on the best-fit nucleotide substitution model determined by the lowest Akaike information criterion value, and the gaps were treated as partial deletion with a 95% site coverage cut-off. ML tree was inferred using the Nearest-Neighbor-Interchange method as a heuristic method, and a neighbor-joining starting tree automatically generated by the MEGA 11.0.10 software. The relative robustness of the clades was assessed by performing 1000 bootstrap replicates.

Determination of growth rates of marine fungal isolates under seawater and distilled water medium conditions

The growth rate of fungi is commonly determined through measuring the colony diameter on the agar plate²⁴. In the present study, daily diametric measurements of the colonies were done. Each of the eight fungal isolates were cultivated in media with and without artificial saltwater to assess whether the absence of salt in the growth medium could act as a hypo-osmotic stressor with potential benefits to produce metabolites capable of reducing, capping and stabilizing AgNPs. Specifically, each fungal species was inoculated in malt extract, yeast extract, glucose, and peptone (MYGP) agar medium [agar (15 g/L; Liofilchem), malt extract (3 g/L; VWR Chemicals), yeast extract (3 g/L; VWR Chemicals), glucose (10 g/L; Biochem Chemopharma, France), peptone (5 g/L; VWR Chemicals)] prepared either with artificial seawater (sSW) or distilled water (sDW). The artificial seawater was prepared with Sea Salt Instant Ocean (Aquarium Systems Inc., Atlanta, Georgia, USA) at 35 parts per thousand (ppt) with ultrapure water. The experiment was carried out in triplicates. All the plates were incubated at 28 °C, in the dark, for ten days.

Production of cell-free filtrates (CFFs)

After ten days of incubation, seven mycelial plugs were detached from the actively growing edge of each culture (eight in sSW and eight in sDW) and inoculated in 100 mL of MYGP broth [malt extract (3 g/L; VWR Chemicals), yeast extract (3 g/L; VWR Chemicals), glucose (10 g/L; Biochem Chemopharma), peptone (5 g/L; VWR Chemicals)] prepared either with distilled water or artificial seawater, correspondent to the growth in the agar medium (16 flasks in total). The fungal isolates were incubated at 28 °C, 130 rpm for 72 h. After this period, the biomass of each strain was harvested in aseptic conditions by filtration through sterile muslin and washed with sterile ultrapure water to eliminate or reduce the components of the medium in the following steps. Each mycelia biomass was then suspended in 100 mL sterile ultrapure water and incubated at 28 °C, 130 rpm for 72 h. Afterwards, the cell-free filtrates (CFFs), containing the biomolecules produced by the fungi, were obtained by further filtering the liquid culture of each isolate through sterile muslin, while discarding the fungal biomass. The CFFs were then subjected to centrifugation at 3200 g for 30 min at 4 °C followed by a subsequent filtration using 0.22 µm syringe filters. The CFFs were stored at -80 °C until further analysis.

AgNPs biosynthesis and optimizations through the Response Surface Methodology (RSM)

The AgNPs biosynthesis optimization process was carried out using the Response Surface Methodology (RSM) with a Box-Behnken experimental design. This methodology enables the simultaneous evaluation of multiple variables, minimizing the number of experiments required, and optimizing the conditions for synthesizing AgNPs with ideal yield, size, and stability. The optimization process, done in 500 µL reactions, was performed with four out of the sixteen produced CFFs, in two separated RSM experiments, both using Box-Behnken experimental designs, testing five independent variables for each one: pH (5, 7.5, and 10; adjusting the pH of the CFFs with sodium hydroxide and hydrochloric acid), temperature (50, 75, and 100 °C), reaction time (30, 105, and 180 min), silver nitrate concentration (AgNO_3 ; 0.25, 0.875, and 1.5 mM), and CFF concentration in the 500 µL reaction (25, 42.5, and 60% v/v) (Supplementary Table 1). Firstly, pH, temperature, and reaction time were evaluated in RSM1 and then AgNO_3 and CFF, along with reaction time, were evaluated in RSM2. For RSM1, 40% (v/v) of CFF and 1 mM AgNO_3 were fixed and then the optimal settings in terms of temperature and pH obtained from RSM1 were fixed for RSM2. The AgNO_3 stock solution (10 mM; Thermo Fisher Scientific, Waltham, Massachusetts, USA) was prepared in ultrapure water. A negative control (distilled water at pH 10 instead of CFF) was run for every condition tested. Preliminary confirmation of AgNPs production was done by visual observation of the color change, followed by a UV-Vis spectrometry analysis (Synergy H1 Multimode Reader, BioTek, Winooski, Vermont, USA) at a wavelength range between 300–700 nm to determine their surface plasmon resonance peaks with 10 nm reading gaps at room temperature (RT). The presence of a clear and defined localized surface plasmon resonance (LSPR) peak in the region between 400 and 450 nm indicates AgNPs synthesis. The absorbance at maximum peak as well as the wavelength at maximum peak for each run of the RSMs were the response parameters used as output for the models, serving as an indication for the relative concentration and size of the synthesized AgNPs, respectively. To verify that the tested conditions, particularly those closest to the optimal ones predicted by the models, contributed to nanoparticle stabilization, the stability of the biosynthesized AgNPs was assessed by storing the samples at room temperature for 48 h. Samples that showed no visible precipitate after this period were considered stable.

After optimization, all 16 CFFs were used for the AgNPs biosynthesis reactions under the optimal conditions (pH 10, 100 °C, 105 min, 1.5 mM AgNO_3 , and 40% v/v CFF), in a 500 µL reaction volume. A negative control (distilled water at pH 10 instead of CFF) was run for every condition tested. The reactions of the CFFs that produced better results were selected for further characterization, in triplicates. Data treatment of the results (mean ± standard deviation) of AgNPs absorbance was done on BioTek Gen5 software (version 3.02, BioTek).

AgNPs characterization

Based on UV-Visible analysis, the samples of synthesized AgNPs that demonstrated higher absorbances and peak wavelengths close to 400 nm (indicative of theoretically smaller nanoparticles) were selected for further

characterization. Triplicates of the five selected AgNPs (AgNPs biosynthesized by the CFFs of *Talaromyces pinophilus*, *Aspergillus fructus*, *Purpureocillium lilacinum*, *Penicillium toxicarium*, and *Emericellopsis maritima*) were separated by a centrifugation process at 20,500 g for 1 h at RT, redispersed in 500 μ L of ultrapure water, and pooled for further characterization (5 pooled samples, from three replicates, one of each fungal CFF). For the analysis of the AgNPs average size (Z-average) and size distribution, a dynamic light scattering (DLS) analysis was performed, enabling the determination of whether the samples have a uniform size distribution (monodisperse) or a broad range of sizes (polydisperse) through the polydispersity index (PdI). AgNPs stability through the zeta potential (ζ -potential) was also determined. A Zetasizer Ultra Red (Malvern Instruments Ltd., United Kingdom) was used for the DLS and ζ -potential analysis at 25 °C with a threefold dilution of the samples in ultrapure water. The results were treated on ZS Xplorer (version 3.3.1.5, Malvern Instruments Ltd.). Fourier Transform Infrared spectroscopy (FTIR) analysis was performed in an Alpha-P FTIR (Bruckner, Billerica, Massachusetts, USA) with a resolution of 4 cm^{-1} . The spectrum (wavelength vs transmittance) was recorded between 4000–400 cm^{-1} to identify chemical bonds groups of possible biomolecules involved in the biosynthesis and AgNPs capping and stabilization. The AgNPs morphology, aggregation, and dispersion were examined by scanning electron microscopy (SEM) using Vega3-LMU (TESCAN, Czech Republic). Prior to examination, samples were coated with an Au/Pd thin film by sputtering (Quorum Technologies, UK). Additionally, Energy-Dispersive X-ray (EDX, Bruker Spectroscopy, Xflash 6–30, Würzburg, Germany) was performed to analyze the elemental composition of the synthesized AgNPs.

Statistical analysis

Student t-tests were performed using TIBCO Statistica (version 14.0.0.15, TIBCO Software Inc, Palo Alto, CA, USA), to compare the growth of each marine fungal species in solid culture medium made with distilled water and with artificial seawater, to assess possible hypo-osmotic stress on their growth ($n = 6$, three of hypo-osmotic growth and three of artificial seawater growth—for each tested species). For the optimization of the AgNPs production conditions, two Box-Behnken design experiments were performed for each of the four CFFs tested, resulting in 120 experimental runs (60 runs for each RSM), for which the values of the five variables under study (pH, temperature, reaction time, AgNO_3 concentration, and CFF concentration), and the values for each of the two parameters determined (absorbance and wavelength at maximum peak) were organized in different tables. For each Box-Behnken experiment, eight response surface models were computed (four CFFs \times two output parameters; sixteen models in total), using TIBCO Statistica (version 14.0.0.15). The goodness-of-fit statistical parameters (sum of squares, adjusted R-squared, p-value, and degrees of freedom) are reported alongside the contour plots for each fitted model. In some cases, $2 \times$ or $4 \times$ dilutions of the reaction products were performed to allow the measurement on the UV–Vis and for the modelling purposes these absorbance outputs were then multiplied by their respective dilution factor. Where applicable, the data were expressed as mean \pm standard deviation and for all statistical tests, the significance level was set at $p \leq 0.05$. Contour-plots were done on TIBCO Statistica (version 14.0.0.15). GraphPad Prism (version 8.0.2.263, Boston, Massachusetts, USA) was used for the graphics related to the fungal growth rates and AgNPs characterization results.

Results

Identification of marine endophytic fungi

The DNA sequences of the isolates were deposited in the NCBI database under the accession numbers PQ591461–PQ591467, PV393045–PV393047, and PV418101–PV418102. The molecular approach enabled the identification of the eight selected fungal strains to the species level: *T. pinophilus*, *A. fructus*, *Stemphylium gracilariae*¹⁶, *P. lilacinum*, *Microascus croci*, *P. toxicarium*, *Exophiala mesophila*, and *E. maritima* (Supplementary Table 2, 3, and 4). The multilocus phylogenetic tree generated by ML analysis regarding *M. croci* is shown in Supplementary Fig. 1. All the identified fungal taxa are included in the phylum Ascomycota.

Effects of hypo-osmotic conditions on the growth of marine fungal isolates

The growth rates of the fungal isolates in the presence and absence of salinity were determined for seven out of the eight species (Fig. 1). The growth rate of *E. mesophila* was not calculated due to its irregular and non-radial growth pattern. Significant statistical differences were observed in the growth rates of five species (*A. fructus*, *S. gracilariae*, *P. lilacinum*, *M. croci*, and *E. maritima*). The growth rates were higher in the presence of salinity, in contrast to *P. lilacinum* (Supplementary Table 5). Besides the differences in growth rates, different pigmentation or morphology were also observed for those five species (Supplementary Fig. 2).

AgNPs biosynthesis and reaction optimization studies

The RSM optimization procedures were performed with four different CFFs (*A. fructus* SW, *T. pinophilus* DW, *P. lilacinum* DW, and *E. maritima* DW) resulting in eight models for each RSM (two output parameters) and 16 models in total. However, in the case of *E. maritima* DW CFF, the conditions tested in the second RSM did not produce enough differences in the UV–Vis spectra profile to allow for an adjustment of the model. The goodness-of-fit and statistical parameters for each of the fourteen remaining models can be found on Supplementary Table 6.

Regarding the first optimization (RSM1), the contour plots resulting from the models with higher regression coefficients can be seen in Fig. 2, specifically the best fitted model for absorbance at maximum peak (Fig. 2a–c) and for wavelength at maximum peak (Fig. 2d–e) according to the three tested variables (pH, temperature, and reaction time). Regarding absorbance at maximum peak (OD_{max}) as an indication of AgNPs relative concentration, results of the models showed that time had little influence on the biosynthesis reactions and that temperature and especially pH were the main drivers influencing the increase in absorbance with higher pH values and higher temperature settings improving the relative concentration of AgNPs (Fig. 2a–c; Suppl. Table

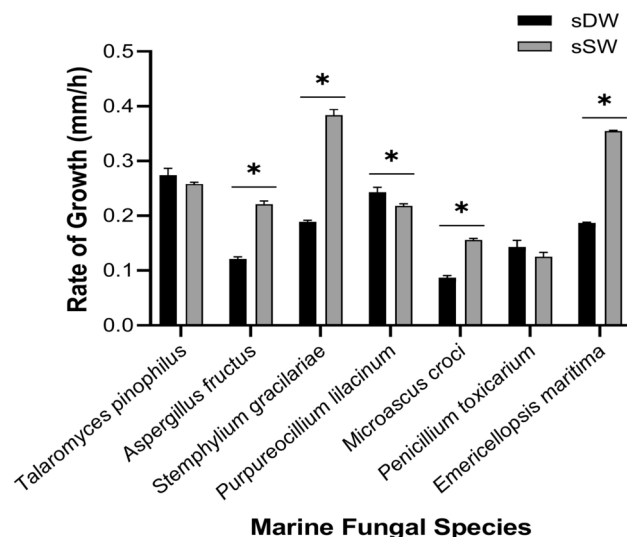


Fig. 1. Fungal growth rate in millimeters per hour (mm/h) of *Talaromyces pinophilus*, *Aspergillus fructus*, *Stemphylium gracilariae*, *Purpureocillium lilacinum*, *Microascus croci*, *Penicillium toxicarium*, and *Emericellopsis maritima*, with daily measurements taken for ten days. Black bars represent fungal isolates cultured on solid medium with distilled water (sDW) and grey bars represent fungal isolates cultured on solid medium with artificial seawater (sSW). Student t-tests were performed and * represents statistically significant differences between culturing conditions for each fungal isolate ($p \leq 0.05$).

6). As for the wavelength at maximum peak (λ_{\max}), as an indication of the AgNPs' theoretical size, the same observations could be made with especially higher pH producing a shift of the absorbance peak to the left of the spectra, closer to 400 nm (Fig. 2d–f; Suppl. Table 6). Overall, after the experiments of RSM1, the results of the models led to the decision to fix the temperature at 100 °C and pH 10 for the second Box-Behnken design. The contour plots for the best fitted models after the second optimization (RSM2) are also seen in Fig. 2, with the best fitted model for absorbance at maximum peak in graphs g–i and best fitted model for wavelength at maximum peak in graphs j–l, according to the three tested variables (AgNO₃ concentration, CFF concentration, and reaction time). The results pointed to a clear and main influence of AgNO₃ concentration in the absorbance values of AgNPs, with higher concentrations of the metal salt producing higher absorbance values (Fig. 2g, h; Suppl. Table 6). This combination of conditions also showed that reaction times longer than 90 min are more likely to produce theoretical smaller nanoparticles. As the reaction time increases, the absorbance peaks shift closer to 400 nm (Fig. 2k, l; Suppl. Table 6).

Based on the overall results of all the optimization experiments with the four different CFFs, it was possible to set the optimal conditions for AgNPs biosynthesis as: pH 10, 100 °C, 105 min, 1.5 mM AgNO₃ and 40% (v/v) of CFF. To note that all AgNPs synthesized with those conditions in the RSM experiments were considered stable. Having this information, all 16 produced CFFs (eight species cultured in DW plus the same eight species cultured in SW), were used for new biosynthesis reactions under the optimal conditions and the UV–Vis spectrum results can be seen in Fig. 3.

From the analysis of the 16 reactions, it is possible to observe that eight of the CFFs had limited or no capacity for AgNPs biosynthesis, namely *T. pinophilus* SW (Fig. 3a), *S. gracilariae* grown at both DW and SW (Fig. 3c), *P. lilacinum* SW (Fig. 3d), and *M. croci*, and *E. mesophila* grown at both DW and SW (Fig. 3e, g). For the remaining CFFs it is also clear that the fungi cultured in distilled water (DW) produced CFFs with higher capacity for AgNPs production in terms of relative concentration, accordingly to the higher absorbance values of the DW CFFs in comparison with the SW CFFs of the same fungi (Fig. 3b, f, h). In fact, for some of the fungal species, only the DW CFF was able to reduce the silver ions, as seen in the case of *T. pinophilus* and *P. lilacinum* (Fig. 3a, d). Moreover, it can also be observed that the DW CFFs generally produced narrower absorbance peaks (an indication of monodispersion) at lower wavelengths (an indication of smaller particles), compared to their SW counterparts (Fig. 3b, f, h). For this reason, the five best performing DW CFFs were chosen for further characterization: *A. fructus* CFF, *P. toxicarium* CFF, *E. maritima* CFF, *T. pinophilus* CFF, and *P. lilacinum* CFF. The CFF of *E. maritima* grown in DW was the one producing a narrower absorbance peak and with higher absorbance values (Fig. 3h). The summary table of the AgNPs biosynthesis by all cell-free filtrates alongside the marine fungi growth rates is shown in Supplementary Table 7.

AgNPs characterization

The UV–vis spectrum of the new AgNPs biosynthesis reactions with the selected CFFs, in triplicates, is shown in Fig. 4.

Having into consideration the dilution factors applied for the spectrophotometric analysis, *E. maritima* DW CFF produced the higher relative concentration of AgNPs (higher absorbance values at maximum peak) followed by *P. lilacinum*, *A. fructus*, *P. toxicarium*, and *T. pinophilus*. All CFFs produced peaks of absorbance

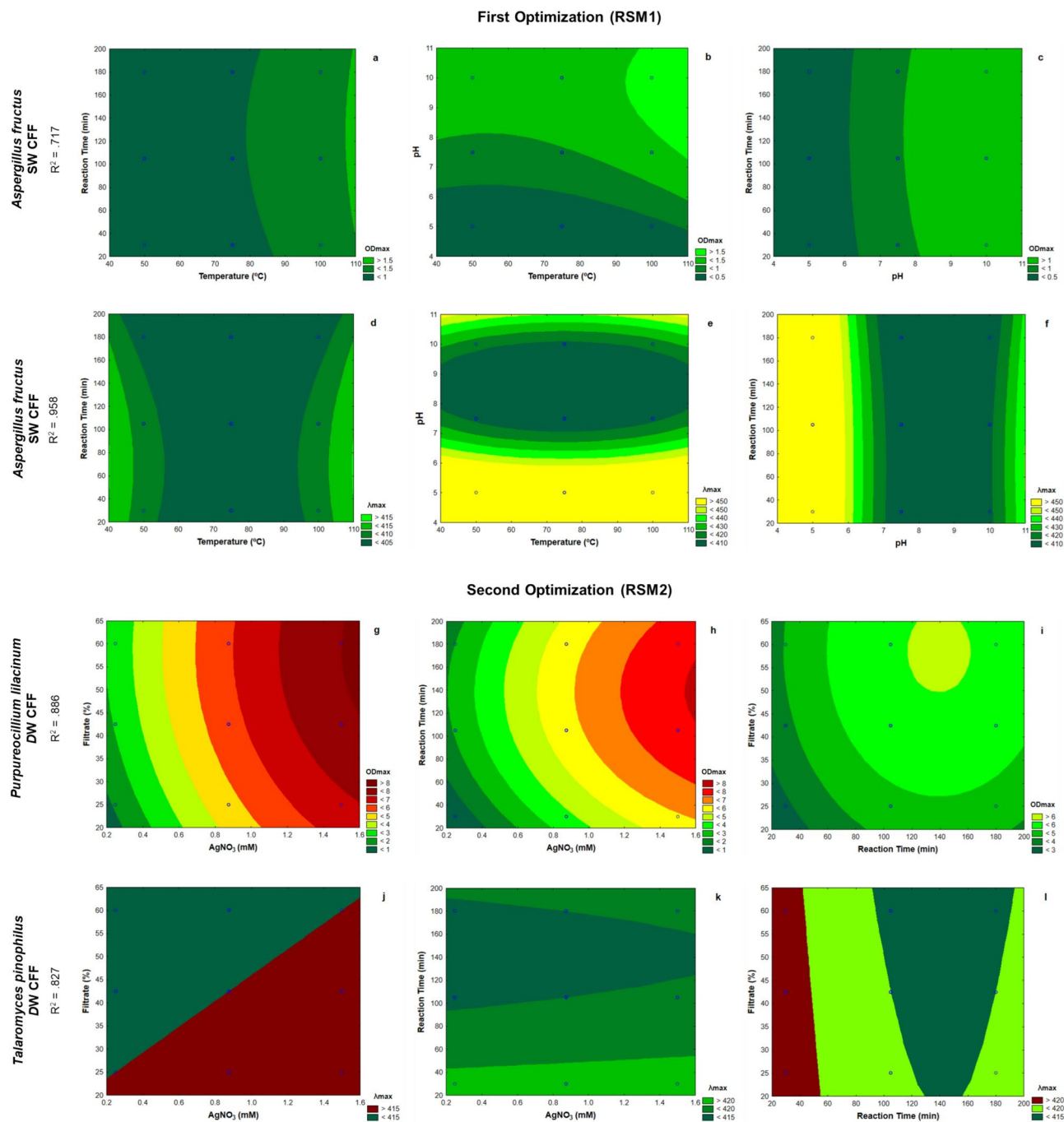


Fig. 2. Contour plots of the modelled function regarding the absorbance at maximum peak (OD_{max}) and wavelength at maximum peak (λ_{max}) obtained for the first Response Surface Methodology (RSM) optimization (RSM1; **a–f**) regarding the variables temperature, pH, and reaction time, and the second RSM optimization (RSM2; **g–l**) regarding the variables silver nitrate (AgNO₃) concentration, and reaction time, in the reactions of silver nanoparticles (AgNPs) biosynthesis using a Box–Behnken design. Only the models with higher regression coefficients are presented, namely the one with *Aspergillus fructus* grown in seawater medium (SW) CFF for RSM1 regarding OD_{max} (**a–c**) and λ_{max} (**d–f**), *Purpureocillium lilacinum* grown in distilled medium (DW) CFF for RSM2 regarding OD_{max} (**g–i**) and *Talaromyces pinophilus* DW CFF for RSM2 regarding λ_{max} (**j–l**).

between 410–420 nm, with *E. maritima* DW and specially *A. fructus* DW having peak maximum at 410 nm slightly more to the left of the wavelength spectrum indicative of smaller nanoparticles and *T. pinophilus* DW at 420 nm more to the right and indicative of larger nanoparticles.

The purification process of the produced AgNPs resulted in a reduction of relative concentration of around 30 to 44% (Supplementary Table 8). However, despite the decrease in the overall absorbance levels, the UV–Vis

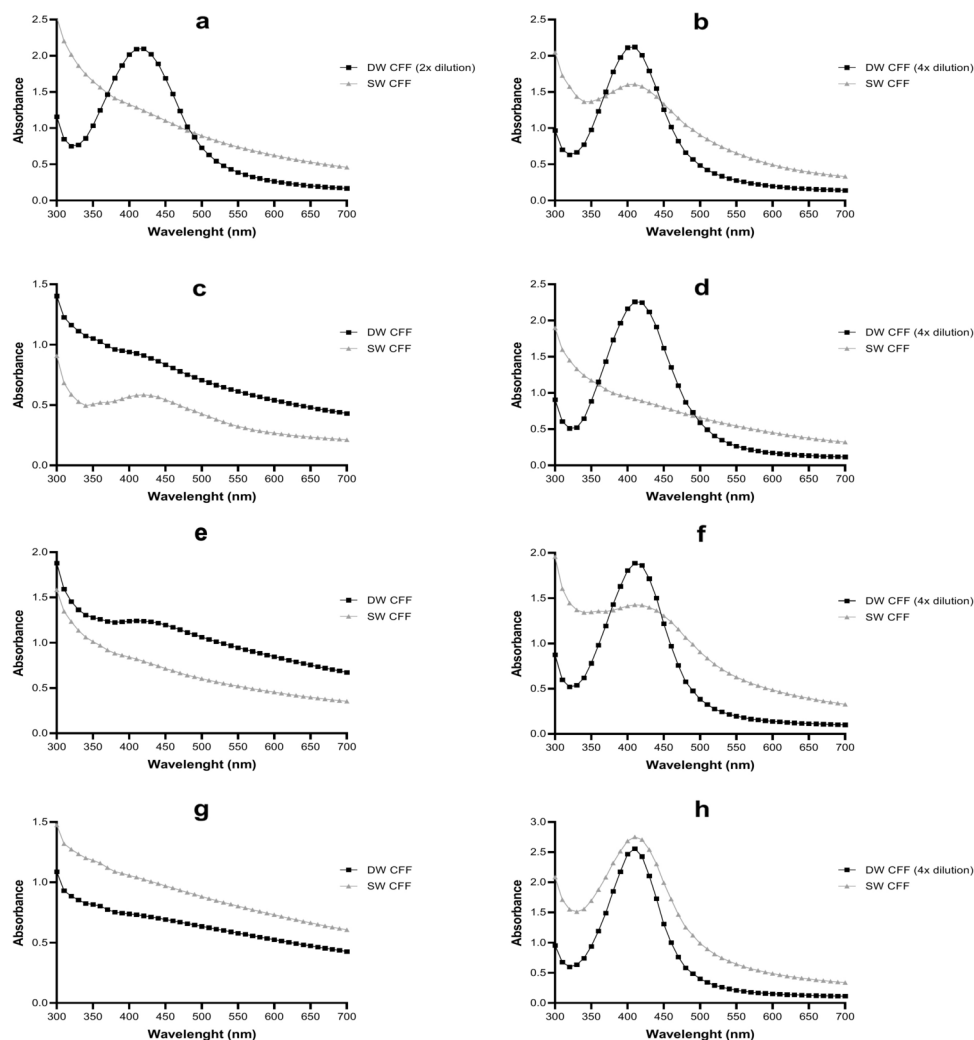


Fig. 3. UV-visible or surface plasmon resonance (SPR) spectrum of the silver nanoparticles (AgNPs) biosynthesized by distilled water (DW, black squares) and artificial seawater (SW, grey triangles) grown fungi cell-free filtrates (CFF) of *Talaromyces pinophilus* (a), *Aspergillus fructus* (b), *Stemphylium gracilariae* (c), *Purpureocillium lilacinum* (d), *Microascus croci* (e), *Penicillium toxicarium* (f), *Exophiala mesophila* (g), and *Emericelopsis maritima* (h).

spectrum curves after purification exhibited similar profiles, apart from *P. lilacinum* DW CFF that exhibited a wider curve (Supplementary Fig. 3).

Average nanoparticle size (Z-average) and polydispersity index (PdI) values retrieved from the dynamic light scattering (DLS) analysis, as well as the zeta-potential (ζ -potential) of the synthesized particles, are demonstrated in Figs. 5 and 6, respectively.

Regarding particle size, it is possible to observe that the frequency of sizes varied in the different samples, characterized by a wide range of PdI values between 0.235 ± 0.067 (*E. maritima* DW CFF) and 0.622 ± 0.161 (*P. lilacinum* DW CFF) (Fig. 5). The CFF of *A. fructus* grown in DW produced the particles with the smallest average size (40.64 ± 2.65 nm) and *P. lilacinum* DW CFF produced the particles with the largest average size (191.60 ± 8.07 nm) (Fig. 5). It can also be highlighted that, although the average size is larger than in the case of *A. fructus* DW CFF, the CFF of *E. maritima* grown in DW was the one producing the higher frequency of the smallest size group particles (0–25 nm) (Fig. 5). As for the ζ -potential, all biosynthesized AgNPs presented values below -20 mV, with *E. maritima* DW CFF and *P. lilacinum* DW CFF producing the particles with the lowest (-28.1 mV) and highest (-24.2 mV), respectively (Fig. 6).

Regarding the FTIR analysis, the main peaks representing chemical components that could be involved in AgNPs synthesis and capping, were detected from the surface of the AgNPs produced with all five fungal DW CFFs and are demonstrated in Fig. 7. The peak wavelengths of each sample, along with their possible corresponding chemical bonds and functional groups are given in Supplementary Table 9.

Similar FTIR spectra were detected for all analyzed samples, although the exact same 10 peaks at similar wavenumbers were only detected for *P. toxicarium* and *E. maritima* DW CFFs (Fig. 7d, e; Suppl. Table 9). Moreover, the AgNPs synthesized from *P. lilacinum* DW CFF did not present the peak possibly related with

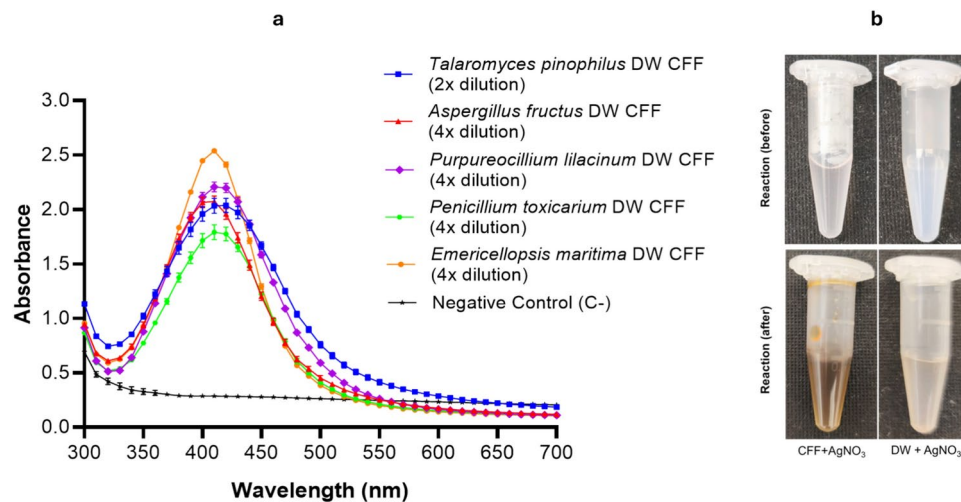


Fig. 4. UV-visible spectrum (a) of silver nanoparticles (AgNPs) biosynthesized by the cell-free filtrates (CFFs) of *Talaromyces pinophilus* (blue), *Aspergillus fructus* (red), *Purpureocillium lilacinum* (purple), *Penicillium toxicarium* (green), and *Emericellopsis maritima* (orange) grown in distilled water (DW) medium. Samples were run with a negative control (distilled water plus AgNO₃; black). The error bars represent standard deviation for each average absorbance point. A visual example of the before and after the *Aspergillus fructus* CFF AgNPs biosynthesis in comparison to the negative control is also shown (b).

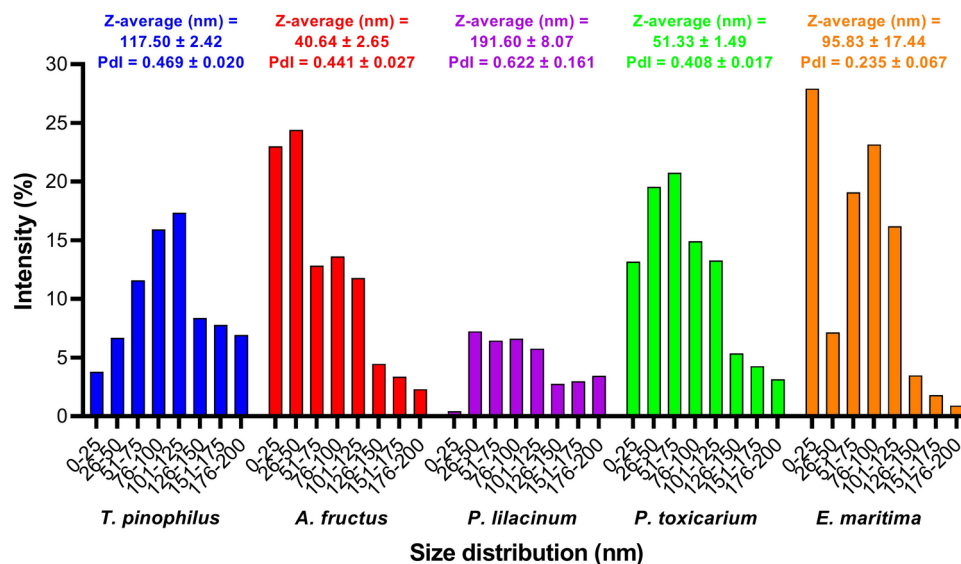


Fig. 5. Size distribution (nm) versus intensity (%) in the dynamic light scattering (DLS) analysis for the silver nanoparticles (AgNPs) biosynthesized by the *Talaromyces pinophilus* (blue), *Aspergillus fructus* (red), *Purpureocillium lilacinum* (purple), *Penicillium toxicarium* (green), and *Emericellopsis maritima* (orange) cell-free filtrates (CFF) of the fungi grown in distilled water (DW) medium. Respective average nanoparticle size (Z-average) and polydispersity index (PDI) values are reported on top of each group.

a O–H stretching bond as all the others (Fig. 7c; Suppl. Table 9), while the peak related to possible S–S/S–S stretching/C–Br bonds was also undetected for *T. pinophilus* and *A. fructus* samples (Fig. 7a, b; Suppl. Table 8). Overall, similar functional groups may be involved in the AgNPs synthesis and capping by the analyzed CFFs (Suppl. Table 9).

The morphological analysis of the particles, performed by scanning electron microscope (SEM), can be seen in Fig. 8. AgNPs are generally well dispersed and possess varied shapes for example, spherical, quasi-spherical, star-shape, polyhedral shapes (e.g., cube, pentagon...), rod-like shape and others. Almost all CFFs synthesized spherical and quasi-spherical AgNPs, although star-shape AgNPs could be observed for *T. pinophilus* (Fig. 8a), polyhedral shapes for *P. lilacinum* (Fig. 8c), and rod-shape for *E. maritima* (Fig. 8e). Also, from the SEM analysis it can be observed that, under this magnification, the density of the AgNPs from *T. pinophilus* DW CFF seems

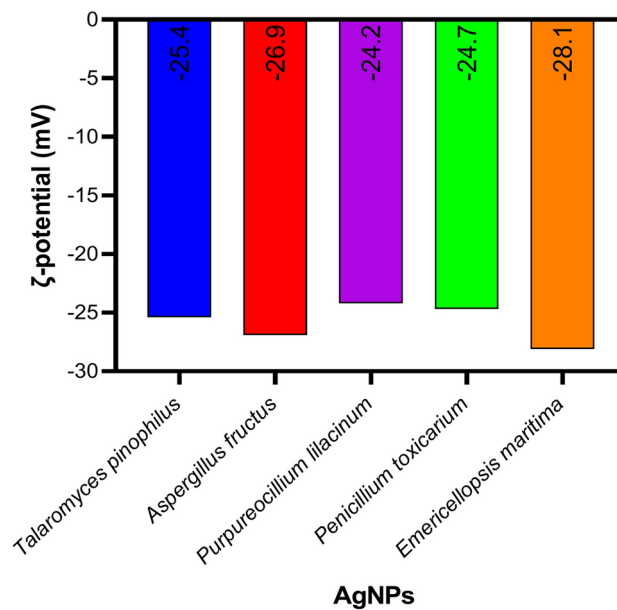


Fig. 6. Zeta potential [ζ -potential; milivolts (mV)] for the biosynthesized silver nanoparticles (AgNPs) of *Talaromyces pinophilus* (blue), *Aspergillus fructus* (red), *Purpureocillium lilacinum* (purple), *Penicillium toxicarium* (green), and *Emericellopsis maritima* (orange) cell-free filtrates grown in distilled water medium.

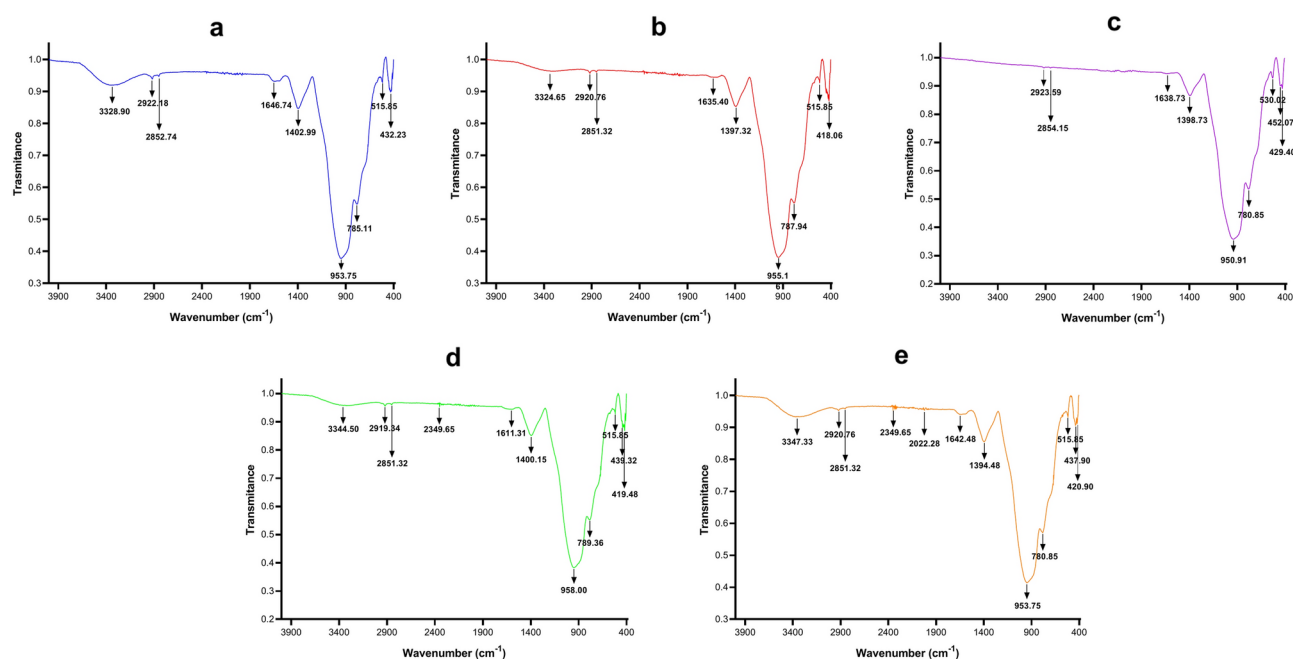


Fig. 7. Fourier-transform infrared spectroscopy (FTIR) spectrum and the detected peaks of the surface of biosynthesized silver nanoparticles (AgNPs) from the cell-free filtrates of *Talaromyces pinophilus* (blue, a), *Aspergillus fructus* (red, b), *Purpureocillium lilacinum* (purple, c), *Penicillium toxicarium* (green, d), and *Emericellopsis maritima* (orange, e) grown in distilled water medium. Different peaks in the graph may indicate the presence of different functional groups.

to be lower and the AgNPs of *P. lilacinum* DW CFF appear to be bigger in size than all the other (Fig. 8a, c). Even though all AgNPs seem to be generally monodispersed, those AgNPs of *T. pinophilus*, *P. lilacinum* and *E. maritima* seemed to have more aggregates (Fig. 8a, c, e). Energy-dispersive X-ray spectroscopy (EDX) analysis confirmed the presence and relative concentration of silver in the biosynthesized nanoparticles (Supplementary Fig. 4).

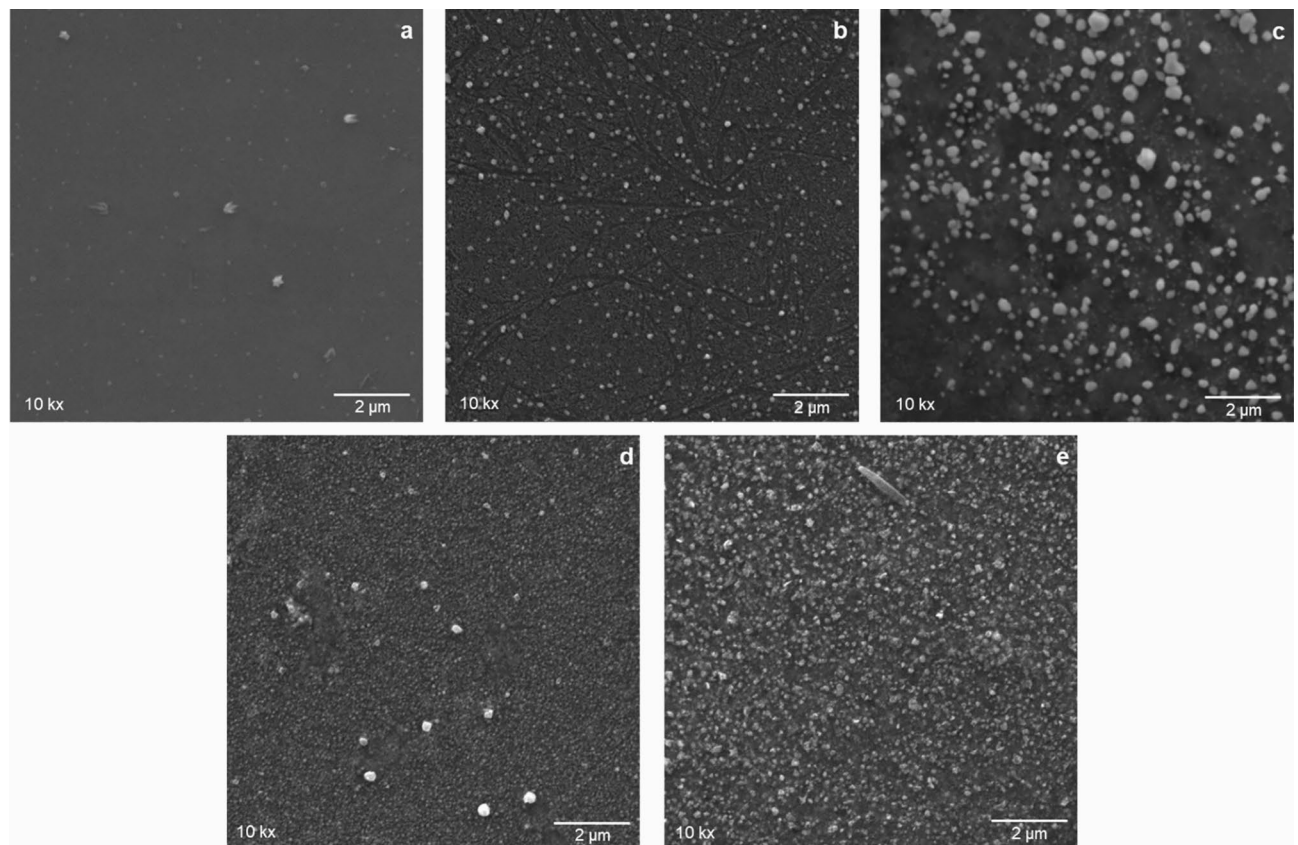


Fig. 8. Scanning electron microscope (SEM) images of the biosynthesized silver nanoparticles (AgNPs) by the cell-free filtrates of *Talaromyces pinophilus* (a), *Aspergillus fructus* (b), *Purpureocillium lilacinum* (c), *Penicillium toxicarium* (d), and *Emericellopsis maritima* (e) on a scale of 2 μ m with a 10 k magnification.

Discussion

All the identified fungal species belonged to the phylum Ascomycota, confirming the dominance of this phylum in marine environments and its frequent occurrence as endosymbiotic partner of seaweed, as demonstrated in previous studies²⁵.

Six fungal species have been previously reported from marine ecosystems, but only three of these as endophytes of seaweed. Specifically, *S. gracilariae* was recovered from *Gracilaria* sp.²³, *T. pinophilus* from an unidentified seaweed²⁶, and *M. croci* from a brown seaweed (*Desmarestia anceps* Montagne 1842)²⁷. Even though *A. fructus*, *E. maritima* and *P. lilacinum* had been retrieved from the internal tissues of different marine hosts, this is the first report of these species as endophytes of seaweed. The sea cucumber *Holothuria poli* has been found to host *A. fructus* as an endobiont on only one occasion²⁸. The cosmopolitan black yeast-like fungus *E. mesophila* was recently isolated from deep-sea sediments²⁹, thus this study represents the first report of this species occurring within seaweed. The species *T. pinophilus* was found associated with the sponge *Mycale* sp.³⁰ and mangrove sediments^{31,32}. The species *P. lilacinum* has been isolated from marine sea cucumber *Holothuria poli*²⁹, *Stylissa* sp. sponge³³, and marine sediments³⁴. Also, *E. maritima* has been found in marine sediments^{34,35} and driftwood³⁶. The identification of these species in various ecological niches, each employing different nutritional strategies, underscores their metabolic versatility and ability to adapt to a wide range of environmental conditions.

The optimal production conditions for AgNPs biosynthesis varies with the fungal species. Distinct species may exhibit different metabolic pathways and responses to stress, which will reflect on their ability to produce certain biomolecules⁷.

Among all the tested variables, pH, temperature, and AgNO₃ concentration were the ones with a greater impact on the relative concentration and AgNPs theoretical size. pH is known to influence AgNPs mainly by changing the shape of the biomolecules and consequently their capping and stabilizing capacities¹². An alkaline pH improves AgNPs biosynthesis yields, growth, and stability³⁷ and can also speed up the reaction time. However, in the present study, the relationship between reaction time and pH did not have a major impact on the quantity of AgNPs or the peak wavelengths values⁶. The optimization models applied in this study revealed that higher alkaline pH values were associated with higher absorbance peaks and lower wavelengths, which are common indicators of higher relative concentrations of small sized nanoparticles. This finding aligns with a previous study by³⁸ using cell-free filtrates (CFFs) of the marine isolated fungi *Aspergillus niger*, and other studies from non-marine fungi, that obtained higher AgNPs concentrations at pH levels ranging from 9 to 12 higher^{7,39,40}. These and other studies have also shown that lower pH values can lead to the formation of larger nanoparticles,

potentially due to nanoparticle aggregation or agglomeration^{39–41}. Temperature is another factor known to impact the size and stability of AgNPs⁶. According to these study models, elevated temperatures promoted higher absorbance levels, lower wavelengths at maximum peak, and apparent better stabilities, which were similar results to other studies with different non-marine and marine fungal species^{7,42,43}. It is proposed that enzymes and/or other proteins produced by the biological systems play a vital or main role in the mechanism of reduction and stabilization of AgNPs, including those biosynthesized by marine fungi⁴⁴. However, at elevated temperatures (as 100 °C, used in this study), native proteins including enzymes go through a process of denaturation, unfolding and, possible degradation⁴⁵. Therefore, at these temperatures it is unlikely that enzymes will be the active agents associated with the AgNPs biosynthesis process⁷. However, it is not surprising that enzyme reduction is the most consensual theory since in most studies the temperatures used in fungal AgNPs synthesis ranged from 20 to 60 °C, and only very few applied temperatures above that range^{14,43,46}. In addition to pH and temperature, the concentration of the metal precursor also influenced the concentration of AgNPs. Most studies of extracellular AgNPs biosynthesis use 1 mM AgNO₃ (reviewed by⁶), but others have shown that using higher concentrations of AgNO₃ directly improves the concentration of AgNPs^{12,47,48}. The present work agrees with those assumptions.

Regarding other factors, the concentration of cell-free filtrate (CFF) can also have a direct effect on the concentration of AgNPs synthesized, although the effect was not so evident in this study. In fact, and even though⁴⁷ observed optimal AgNPs concentration with 60% (v/v) fungal CFF (*Aspergillus fumigatus*), in the present study there were no clear improvements with the increase of CFF concentration at a concentration of 40% (v/v), showing that at this concentration the biomolecules present were present in enough concentration to reduced and stabilize AgNPs even at the maximum AgNO₃ tested (1.5 mM). Besides the use of distinct species, the reaction temperature also differed between this and the mentioned study, which may explain the differing results. These authors used 30 °C and the results from this work clearly showed that higher temperatures improve CFFs' efficiency for AgNPs production. In relation to the time of reaction, this parameter differs highly from study to study, and it is very dependent on the other conditions used. For example, in the present study the results showed that under the optimal conditions of pH, temperature, and AgNO₃ concentration, reaction time had little influence on AgNPs relative concentration, although a period longer than 90 min seems to have some influence on reducing the AgNPs size.

In addition to optimizing reaction parameters, AgNPs purification is a critical step often overlooked in literature. Purification prevents synthesis residues from affecting characterization and applications⁴⁹. In this study, centrifugation and redispersion in ultrapure water caused a loss in relative concentration. Moreover, the UV–Vis spectra maintained general profiles but showed lower absorbances, with *P. lilacinum* DW CFF indicating possible nanoparticle aggregation. However, since most studies do not report UV–Vis results post-purification, it is unclear if this is a common phenomenon. To mitigate the loss concentration purification could be improved by using techniques such as ultracentrifugation, density gradient centrifugation, or differential centrifugation^{50,51}.

The results of the growth experiment revealed different patterns, depending on the species. The higher/more significant differences in the growth rate between media were seen for the remaining tested species (*A. fructus*, *S. gracilariae*, *M. croci*, and *E. maritima*). The significantly slower growth of these species in the DW medium (hypo-osmotic conditions) suggests that the absence of salinity may act as a stress factor. Osmotic stress is known to cause changes at the phenotypical, molecular, and metabolic level of different fungal species⁵². For example, a study found that changing water potential affected the growth of the marine fungus *Fusarium solani*, hypothesizing that the fungi's physiological mechanisms enable their survival in environments with low water potential conditions⁵³.

The growth differences among fungal isolates under hypo-osmotic conditions may derive from their metabolic versatility, allowing stress adaptation. These conditions may favor AgNPs production, as most filtrates from fungi grown under hypo-osmotic stress were more efficient in AgNPs biosynthesis. Not all fungal species could reduce the silver ions, even when cultured under those conditions (*S. gracilariae*, *M. croci*, and *E. mesophila*). Notably, *S. gracilariae* and *M. croci* were affected by hypo-osmotic stress yet showed lower AgNPs production. It is known that species under stress, attempting to adapt to new environmental conditions, are more likely to produce a broader range of biomolecules⁴⁵, which can, in turn, enhance nanoparticle reduction and stability. Even other species, not showing stress signs, could be producing biomolecules that facilitate silver ion reduction without compromising growth. Exposing microorganisms to stressful conditions during their growth phase may be beneficial as shown by⁵⁴. The authors exposed *Deinococcus radiodurans* to metal stress, hypothesizing that stress-induced defense mechanisms promote AgNPs production, resulting in higher concentrations, better homogeneity, and smaller sizes. However, further research is needed to explore how stressors during fungal culturing affect nanoparticle biosynthesis.

Moreover, further analysis of the CFFs, such as gas chromatography mass spectrometry or high-performance liquid chromatography techniques, would provide valuable insights into the chemical composition of those fungal filtrates and help to identify and quantify the biomolecules that may be involved in this higher performance. This would be particularly relevant to apply to CFFs of *T. pinophilus* and *P. lilacinum*, considering that only those who originated from the DW medium were able to produce AgNPs. According to the FTIR analysis performed in this study, several functional groups of possible biomolecules, such as alcohols, phenols, alkanes, aldehydes, amines, carboxylic, ether, disulfides or alkyl halides, may be involved in the biosynthesis, stabilization, and capping functions of AgNPs. These functional groups have been identified in studies performed with marine fungal species^{12,13,43,46,55,56}. AgNPs from *P. lilacinum* DW CFF lacked the O–H stretching peak, while *T. pinophilus* and *A. fructus* DW CFFs only showed two out of three peaks for S–S/C–Br bonds. This suggests different compounds may have been used for nanoparticle reduction and stabilization. However, the FTIR results could have been influenced by the non-homogeneous distribution of AgNPs on the coverslip.

DW CFFs	UV–Visible ^(a)	DLS		ζ-potential ^(d)	SEM/EDX	
		Z-average ^(b)	PdI ^(c)		SEM	EDX
<i>Aspergillus fructus</i>	+++	+	Highly polydisperse	Moderately stable	Mostly spherical or quasi-spherical AgNPs	Silver presence confirmed
<i>Emericellopsis maritima</i>	+++++	+++	Moderately dispersed			
<i>Penicillium toxicarium</i>	++	++	Highly polydisperse			
<i>Purpureocillium lilacinum</i>	+++	+++++				
<i>Talaromyces pinophilus</i>	+	++++				

Table 1. Summary table of the characterization results on the silver nanoparticles synthesized by the cell-free filtrates (CFFs) of the marine fungi *Aspergillus fructus*, *Emericellopsis maritima*, *Penicillium toxicarium*, *Purpureocillium lilacinum*, and *Talaromyces pinophilus* grown under hypo-osmotic conditions (DW) regarding UV-Visible results, nanoparticle average size (Z-average) and polydispersity index (PdI) (dynamic light scattering – DLS), nanoparticle stability (ζ -potential), scanning electron microscope (SEM), and energy dispersive X-Ray (EDX). ^(a)Absorbance at maximum peak from the highest (+++++) to the lowest (+) value. ^(b)Nanoparticle average size from the smallest (+) to the largest (+++++). ^(c)Polydispersity index (PdI) according to ⁵⁸. ^(d)Stability by zeta-potential according to ⁵⁹.

For the AgNPs synthesized using the five best-performing CFFs (all derived from DW medium), EDX analysis confirmed the presence of silver, supporting the UV-vis results, which showed SPR peaks in the 400 nm range. These peaks are primarily associated with spherical AgNPs⁵⁷ and a significant number of spherical or quasi-spherical AgNPs were observed in the SEM images. Although the Ag/C ratio obtained from EDX provides a relative concentration of silver content in the nanoparticles, factors such as sample heterogeneity, matrix effects, and detection limits can affect its accuracy. For future studies on the downstream applications of the biosynthesized nanoparticles, a more precise quantification of silver concentration should be pursued using techniques such as Inductively Coupled Plasma—Mass Spectrometry. The summary table of the characterization results on the AgNPs is shown in Table 1.

The DW CFFs of *T. pinophilus* and *P. lilacinum* produced the largest average size AgNPs as shown by DLS measurements and confirmed by the SEM images, particularly for *P. lilacinum*, exceeding the size defined by the International Organization for Standardization⁶⁰. They also presented the highest polydispersity index (PdI), indicating a wider range of particle sizes, supported by the broader curves on UV-Visible spectra, which suggest the presence of larger agglomerates or aggregates. Their lower absorbance at maximum peak values aligned with the lower AgNPs density seen in SEM images, especially for *T. pinophilus*. Noteworthy, a study by⁶¹ also produced AgNPs using *P. lilacinum*, although isolated from soil and using different synthesis conditions (1 mM AgNO₃, 48 h, and 28 °C), leading to different nanoparticle characteristics. The same was observed in relation to *P. toxicarium*, specifically with a strain isolated from decaying wood, that showed the synthesis of AgNPs with distinct characteristics (larger size, lower PdI, and weaker ζ-potential) as the ones here, while different synthesis conditions were also used (pH 12, 45 °C, 64 h, and 0.25 mM AgNO₃)⁶². These results emphasize how synthesis conditions can significantly influence AgNPs properties.

On the other hand, *A. fructus* DW CFF produced the smallest AgNPs, as shown by the UV-Vis results, with the peak slightly shifted to the left, and confirmed by the DLS analysis and SEM images. The PdI of these AgNPs falls within the polydisperse range according to⁶³. In relation to *E. maritima*, the CFF synthesized the highest quantity of AgNPs, with the lowest PdI (moderately polydisperse)⁵⁸. These findings are consistent with the high density of AgNPs seen in SEM images and the narrower and leftward UV-Visible curve, suggesting low size dispersity and small particles, which could also be seen by the DLS (highest percentage of 0–25 nm size range). These AgNPs were also the most stable according, though still classified as moderately stable⁵⁹. Overall, cell-free filtrates from marine fungi grown under stressful conditions, contributed to a highly efficient biosynthesis of AgNPs with optimal size, monodispersity and stability.

Conclusions

The results obtained in this study demonstrate the potential of using seaweed-associated marine fungi cell-free filtrates (CFFs) to synthesize silver nanoparticles (AgNPs), particularly when the fungi are grown under hypo-osmotic conditions. In this study, the optimization procedures resulted in optimal conditions to increase nanoparticles' relative concentrations and reduce their size, while ensuring stability (pH 10, 100 °C, 105 min, 1.5 mM AgNO₃ and 40% v/v CFF). In particular, the CFFs from *T. pinophilus*, *A. fructus*, *P. lilacinum*, *P. toxicarium*, and *E. maritima* cultured under hypo-osmotic conditions produced higher concentrations of generally monodispersed AgNPs with good stability (zeta-potential bellow – 20 mV) and varying size ranges, achieving high percentages of very small particles (bellow 50 nm). These characteristics of the green AgNPs could be of added value for a range of applications from the healthcare sector to textiles or even to the preservation of cultural heritage materials. Notably, further characterization studies could provide deeper insights into the chemical composition of the fungal filtrates and help identify the specific biomolecules responsible for this enhanced performance. Overall, the results of this study demonstrated the great potential of manipulating fungal culturing conditions during growth to improve the green production of NPs, and further studies exploring different stress conditions could be valuable.

Data availability

The data supporting this article have been included as part of the Supplementary Information and the DNA sequences of the fungal isolates are available on the GenBank database under the accession numbers PQ591461-PQ591467, PV393045-PV393047, and PV418101-PV418102.

Received: 6 January 2025; Accepted: 16 April 2025

Published online: 10 May 2025

References

- Zhang, X. F., Liu, Z. G., Shen, W. & Gurunathan, S. Silver nanoparticles: synthesis, characterization, properties, applications, and therapeutic approaches. *Int. J. Mol. Sci.* **17**, 1–34 (2016).
- Nie, P., Zhao, Y. & Xu, H. Synthesis, applications, toxicity and toxicity mechanisms of silver nanoparticles: A review. *Ecotoxicol. Environ. Saf.* **253**, 1–12 (2023).
- Dhaka, A., Mali, S. C., Sharma, S. & Trivedi, R. A review on biological synthesis of silver nanoparticles and their potential applications. *Results Chem.* **6**, 1–21 (2023).
- Sajid, M. & Plotka-Wasyłka, J. Nanoparticles: Synthesis, characteristics, and applications in analytical and other sciences. *Microchem. J.* **154**, 1–18 (2020).
- Ameen, F., Al-Homaidan, A. A., Al-Sabri, A., Almansob, A. & AlNadhari, S. Anti-oxidant, anti-fungal and cytotoxic effects of silver nanoparticles synthesized using marine fungus *Cladosporium halotolerans*. *Appl. Nanosci.* **13**, 623–631 (2023).
- Guilger-Casagrande, M. & Lima, R. Synthesis of silver nanoparticles mediated by fungi: A review. *Front. Bioeng. Biotechnol.* **7**, 1–16 (2019).
- Alves, M. F. & Murray, P. G. Biological synthesis of monodisperse uniform-size silver nanoparticles (AgNPs) by fungal cell-free extracts at elevated temperature and pH. *J. Fungi.* **8**, 1–14 (2022).
- Gonçalves, M. F. M., Esteves, A. C. & Alves, A. Marine fungi: Opportunities and challenges. *Encyclopedia* **2**, 559–577 (2022).
- Sarasan, M. et al. Marine algicolous endophytic fungi—a promising drug resource of the era. *J. Microbiol. Biotechnol.* **27**, 1039–1052 (2017).
- Calado, M. L. et al. Marine endophytic fungi associated with *Halopteris scoparia* (Linnaeus) Sauvageau as producers of bioactive secondary metabolites with potential dermocosmetic application. *PLoS ONE* **16**, 1–30 (2021).
- Kathiresan, K., Manivannan, S., Nabeel, M. A. & Dhivya, B. Studies on silver nanoparticles synthesized by a marine fungus, *Penicillium fellutanum* isolated from coastal mangrove sediment. *Colloids Surf. B Biointerfaces* **71**, 133–137 (2009).
- Neethu, S. et al. Efficient visible light induced synthesis of silver nanoparticles by *Penicillium polonicum* ARA 10 isolated from *Chetomorpha antennina* and its antibacterial efficacy against *Salmonella enterica* serovar Typhimurium. *J. Photochem. Photobiol. B.* **180**, 175–185 (2018).
- Hulikere, M. M. & Joshi, C. G. Characterization, antioxidant and antimicrobial activity of silver nanoparticles synthesized using marine endophytic fungus-*Cladosporium cladosporioides*. *Process Biochem.* **82**, 199–204 (2019).
- Basheerudeen, M. A. H., Mushtaq, S. A., Soundhararajan, R., Nachimuthu, S. K. & Srinivasan, H. Marine endophytic fungi mediated Silver nanoparticles application in plant growth promotion in *Vigna radiata* L. *Int. J. Nano Dimens.* **12**, 1–10 (2021).
- Liu, D., Coloe, S., Baird, R. & Pedersen, J. Rapid mini-preparation of fungal DNA for PCR. *J. Clin. Microbiol.* **38**, 471 (2000).
- White, T. J., Bruns, T., Lee, S. J. W. T. & Taylor, J. Amplification and direct sequencing of fungal ribosomal RNA Genes for phylogenetics in *PCR protocols: a guide to methods and applications* (ed. Innis, M. A., Gelfand, D. H., Sninsky, J. J. & White, T. J.) 315–322 (Academic Press, 1990).
- Visagie, C. M. et al. Identification and nomenclature of the genus *Penicillium*. *Stud. Mycol.* **78**, 343–371 (2014).
- Yilmaz, N., Visagie, C. M., Houbraken, J., Frisvad, J. C. & Samson, R. A. Polyphasic taxonomy of the genus *Talaromyces*. *Stud. Mycol.* **78**, 175–341 (2014).
- Gonçalves, M. F. M., Vicente, T. F. L., Esteves, A. C. & Alves, A. Novel halotolerant species of *Emericellopsis* and *Parasarocladium* associated with macroalgae in an estuarine environment. *Mycol.* **112**, 154–171 (2020).
- Sandoval-Denis, M. et al. Redefining *Microascus*, *Scopulariopsis* and allied genera. *Pers.: Mol. Phylogeny Evol. Fungi.* **36**, 1–36 (2016).
- Grum-Grzhimaylo, A. A., Georgieva, M. L., Debets, A. J. & Bilanenko, E. N. Are alkalitolerant fungi of the *Emericellopsis* lineage (Bionectriaceae) of marine origin? *IMA Fungus* **4**, 213–228 (2013).
- Siqueira, J. P. Z. et al. Species diversity of *Aspergillus* section *Versicolores* in clinical samples and antifungal susceptibility. *Fungal Biol.* **120**, 1458–1467 (2016).
- Woudenberg, J. H. C., Hanse, B., Van Leeuwen, G. C. M., Groenewald, J. Z. & Crous, P. W. *Stemphylium* revisited. *Stud. Mycol.* **87**, 77–103 (2017).
- Kuribayashi, T., Lankinen, R. & Mikkonen, K. S. A layered solid-state culture system for investigating the fungal growth and decay behaviour on the cellulosic substrate. *J. Microbiol. Methods* **212**, 1–7 (2023).
- Suryanarayanan, T. S. Fungal Endosymbionts of Seaweeds in *Biology of marine fungi - Progress in Molecular and Subcellular Biology* (ed. Raghukumar, C.) 53–69 (Springer Berlin, 2012).
- Myobatake, Y. et al. Pinophilins A and B, inhibitors of mammalian A-, B-, and Y-family DNA polymerases and human cancer cell proliferation. *J. Nat. Prod.* **75**, 135–141 (2012).
- Teixeira, T. R. et al. Characterization of the lipid profile of Antarctic brown seaweeds and their endophytic fungi by gas chromatography–mass spectrometry (GC–MS). *Polar Biol.* **42**, 1431–1444 (2019).
- Marchese, P. et al. Diversity and bioactivity of fungi associated with the marine sea cucumber *Holothuria poli*: disclosing the strains potential for biomedical applications. *J. Appl. Microbiol.* **129**, 612–625 (2020).
- Cheng, M., Tang, X., Shao, Z., Li, G. & Yao, Q. Cytotoxic epipolythiodioxopiperazines from the deep-sea-derived fungus *Exophiala mesophila* MCCC 3A00939. *J. Nat. Prod.* **86**, 2342–2347 (2023).
- Machado, F. P. et al. New hybrid phenalenone dimer, highly conjugated dihydroxylated C28 steroid and azaphilone from the culture extract of a marine sponge-associated fungus, *Talaromyces pinophilus* KUFA 1767. *Mar. Drugs* **21**, 1–21 (2023).
- He, F. et al. Secondary metabolites from the mangrove sediment-derived fungus *Penicillium pinophilum* SCAU037. *Fitoterapia* **136**, 1–6 (2019).
- Muwawa, E. M. et al. Isolation, characterization and biotechnological potential of tropical culturable rhizospheric fungi from four mangrove species in Kenya. *Afr. J. Microbiol. Res.* **14**, 541–554 (2020).
- Fadillah, W. N. et al. *In vitro* pancreatic lipase inhibition by marine fungi *Purpureocillium lilacinum* associated with *Stylissa* sp. sponge as anti-obesity agent. *HAYATI J. Biosci.* **29**, 76–86 (2022).
- Perazzoli, G. et al. *Emericellopsis maritima* and *Purpureocillium lilacinum* marine fungi as a source of functional fractions with antioxidant and antitumor potential in colorectal cancer: A preliminary study. *J. Mar. Sci. Eng.* **11**, 1–12 (2023).
- Marchese, P. et al. Fungi populate deep-sea coral gardens as well as marine sediments in the Irish Atlantic Ocean. *Environ. Microbiol.* **23**, 4168–4184 (2021).
- Tibell, S., Tibell, L., Pang, K. L., Calabon, M. & Jones, E. G. Marine fungi of the Baltic Sea. *Mycol.* **11**, 195–213 (2020).

37. Ibrahim, N. H., Taha, G. M., Hagaggi, N. S. A. & Moghazy, M. A. Green synthesis of silver nanoparticles and its environmental sensor ability to some heavy metals. *BMC Chem.* **18**, 1–34 (2024).
38. Vala, A. K. & Shah, S. Rapid synthesis of silver nanoparticles by a marine-derived fungus *Aspergillus niger* and their antimicrobial potentials. *Int. J. Nanosci. Nanotechnol.* **8**, 197–206 (2012).
39. Birla, S. S., Gaikwad, S. C., Gade, A. K. & Rai, M. K. Rapid synthesis of silver nanoparticles from *Fusarium oxysporum* by optimizing physicochemical conditions. *Sci. World J.* **2013**, 1–12 (2013).
40. Patil, H. B. V., Nithin, K. S., Sachidananda, S., Chandrashekara, K. T. & Kumar, B. Y. S. Mycofabrication of bioactive silver nanoparticle: Photo catalysed synthesis and characterization to attest its augmented bio-efficacy. *Arab. J. Chem.* **12**, 4596–4611 (2019).
41. Mousavi, S. S., Ghadam, P. & Mohammadi, P. Screening of soil fungi in order to biosynthesize AgNPs and evaluation of antibacterial and antibiofilm activities. *Bull. Mater. Sci.* **43**, 1–8 (2020).
42. Saxena, J., Sharma, P. K., Sharma, M. M. & Singh, A. Process optimization for green synthesis of silver nanoparticles by *Sclerotinia sclerotiorum* MTCC 8785 and evaluation of its antibacterial properties. *Springerplus* **5**, 1–10 (2016).
43. Al-Khuzai, R. A. H., Aboud, M. K. & Alwan, S. K. Biological Synthesis of Silver Nanoparticles from *Saprolegnia parasitica*. *J. Phys. Conf. Ser.* **1294**, 1–15 (2019).
44. Mistry, H., Thakor, R., Patil, C., Trivedi, J. & Bariya, H. Biogenically proficient synthesis and characterization of silver nanoparticles employing marine procured fungi *Aspergillus brunneoviolaceus* along with their antibacterial and antioxidative potency. *Biotechnol. Lett.* **43**, 307–316 (2021).
45. Bakar, N. A., Karsani, S. A. & Alias, S. A. Fungal survival under temperature stress: A proteomic perspective. *PeerJ* **8**, 1–29 (2020).
46. Bhimba, B. V., Gurung, S. & Nandhini, S. U. Silver nanoparticles synthesized from marine fungi *Aspergillus oryzae*. *Int. J. ChemTech. Res.* **7**, 68–72 (2015).
47. Othman, A. M., Elsayed, M. A., Al-Balakocy, N. G., Hassan, M. M. & Elshafei, A. M. Biosynthesis and characterization of silver nanoparticles induced by fungal proteins and its application in different biological activities. *J. Genet. Eng. & Biotechnol.* **17**, 1–13 (2019).
48. Hodhod, M. S., Gaafar, A. R. Z., AlMunqedhi, B. M., Elzein, A. & Abdelmalik, A. M. Exploitation of mangliculous marine fungi, *Amarenographium solium*, for the green synthesis of silver nanoparticles and their activity against multiple drug-resistant bacteria. *Open Chem.* **22**, 1–16 (2024).
49. Martins, C. S. M., Sousa, H. B. A. & Prior, J. A. V. From impure to purified silver nanoparticles: Advances and timeline in separation methods. *Nanomater.* **11**, 1–32 (2021).
50. Ahmad, B. et al. Phyto-fabrication, purification, characterisation, optimisation, and biological competence of nano-silver. *IET Nanobiotechnol.* **15**, 1–18 (2021).
51. López-Rodríguez, A., Mejía-Uriarte, E. & Sato-Berrú, R. A practical proposal for silver nanoparticles (Ag-NPs) separation by differential centrifugation. *J. Nanoparticle Res.* **24**, 1–11 (2022).
52. Araújo, C. A. Osmotolerance as a determinant of microbial ecology: A study of phylogenetically diverse fungi. *Fungal Biol.* **124**, 273–288 (2020).
53. Llamas, D., de Cara Gonzalez, M., Iglesias Gonzalez, C., Ruiz López, G. & Tello Marquina, J. C. The interactive effects of temperature and osmotic potential on the growth of marine isolates of *Fusarium solani*. *J. Ind. Microbiol. Biotechnol.* **35**, 1405–1409 (2008).
54. Chen, A., Contreras, L. M. & Keitz, B. K. Imposed environmental stresses facilitate cell-free nanoparticle formation by *Deinococcus radiodurans*. *Appl. Environ. Microbiol.* **83**, 1–14 (2017).
55. Thakor, R. et al. Biogenic synthesis of silver nanoparticles mediated by the consortium comprising the marine fungal filtrates of *Penicillium oxalicum* and *Fusarium hainanense* along with their antimicrobial, antioxidant, larvicidal and anticancer potency. *J. Appl. Microbiol.* **133**, 857–869 (2022).
56. Mistry, H., Thakor, R. & Bariya, H. Biogenesis and characterization of proficient silver nanoparticles employing marine procured fungi *Hamigera pallida* and assessment of their antioxidative, antimicrobial and anticancer potency. *Biotechnol. Lett.* **44**, 1097–1107 (2022).
57. Béltéky, P. et al. Are smaller nanoparticles always better? Understanding the biological effect of size-dependent silver nanoparticle aggregation under biorelevant conditions. *Int. J. Nanomedicine.* **16**, 3021–3040 (2021).
58. Ardani, H. K. et al. Enhancement of the stability of silver nanoparticles synthesized using aqueous extract of *Diospyros discolor* Willd. leaves using polyvinyl alcohol. *IOP Conf. Ser. Mater. Sci. Eng.* **188**, 1–5 (2017).
59. Clogston, J. D. & Patri, A. K. Zeta Potential Measurement in *Characterization of nanoparticles intended for drug delivery*, *Methods in Molecular Biology* (ed. McNeil, S. E.) 63–70 (Humana Totowa, 2011).
60. International Organization for Standardization. Nanotechnologies – Vocabulary – Part 1: Core vocabulary <https://www.iso.org/obp/ui/en/#iso:std:iso:80004:-1:ed1:v1:en> (2024).
61. Khan, M. et al. Search for effective approaches to fight microorganisms causing high losses in agriculture: application of *P. lilacinum* metabolites and mycosynthesized silver nanoparticles. *Biomolecules* **12**, 1–12 (2022).
62. Korcan, S. E. et al. Cyto-genotoxicity, antibacterial, and antibiofilm properties of green synthesized silver nanoparticles using *Penicillium toxicarium*. *Microsc. Res. Tech.* **84**, 2530–2543 (2021).
63. Sukweenadhi, J. Scale-up of green synthesis and characterization of silver nanoparticles using ethanol extract of *Plantago major* L. leaf and its antibacterial potential. *S. Afr. J. Chem. Eng.* **38**, 1–8 (2021).

Acknowledgements

This study was supported by the Fundação para a Ciência e a Tecnologia (FCT) through the Strategic Projects granted to MARE (UID/04292/MARE-Centro de Ciências do Mar e do Ambiente), Associated Laboratory AR-NET (<https://doi.org/https://doi.org/10.54499/LA/P/0069/2020>), CDRsp (<https://doi.org/https://doi.org/10.54499/UIDB/04044/2020>), and <https://doi.org/https://doi.org/10.54499/UIDP/04044/2020>, and Associate Laboratory ARISE (LA/P/0112/2020), the grant awarded to Sara Guerreiro (2021.05893.BD) and the funding to Juliana Dias (<https://doi.org/10.54499/CEECINST/00060/2021/CP2902/CT0005>) and Sara Novais (<https://doi.org/https://doi.org/10.54499/CEECINST/00060/2021/CP2902/CT0007>). This study had also the support of national funds through project NANOFILM (CENTRO2030-FEDER-01469100), funded by Sistema de Incentivos à Investigação e Desenvolvimento (COMPETE 2030).

Author contributions

M.A.M.O.: conceptualization, sampling, methodology, investigation, formal analysis, writing—original draft; M.L.C.: methodology, investigation, formal analysis, writing—review and editing; S.F.C.G.: methodology, investigation, writing—review and editing; J.R.D.: writing—review and editing; M.J.C.: resources, writing—review and editing, supervision; P.G.M.: conceptualization, methodology, writing—review and editing. S.C.N.: conceptualization, methodology, investigation, formal analysis, resources, writing—review and editing, supervision, project administration.

Declarations

Competing interests

The authors declare no competing interests.

Additional information

Supplementary Information The online version contains supplementary material available at <https://doi.org/10.1038/s41598-025-98978-x>.

Correspondence and requests for materials should be addressed to S.C.N.

Reprints and permissions information is available at www.nature.com/reprints.

Publisher's note Springer Nature remains neutral with regard to jurisdictional claims in published maps and institutional affiliations.

Open Access This article is licensed under a Creative Commons Attribution-NonCommercial-NoDerivatives 4.0 International License, which permits any non-commercial use, sharing, distribution and reproduction in any medium or format, as long as you give appropriate credit to the original author(s) and the source, provide a link to the Creative Commons licence, and indicate if you modified the licensed material. You do not have permission under this licence to share adapted material derived from this article or parts of it. The images or other third party material in this article are included in the article's Creative Commons licence, unless indicated otherwise in a credit line to the material. If material is not included in the article's Creative Commons licence and your intended use is not permitted by statutory regulation or exceeds the permitted use, you will need to obtain permission directly from the copyright holder. To view a copy of this licence, visit <http://creativecommons.org/licenses/by-nc-nd/4.0/>.

© The Author(s) 2025